Materials Science and Engineering A 527 (2010) 5026–5032

Contents lists available at ScienceDirect

Materials Science and Engineering A

journal homepage: www.elsevier.com/locate/msea

Local plastic strain evolution in a high strength dual-phase steel

H. Ghadbeigi [a,*], C. Pinna [a], S. Celotto [b], J.R. Yates [a]

[a] The University of Sheffield, Department of Mechanical Engineering, Mappin Street, Sheffield S1 3JD, UK
[b] Corus RD&T, IJmuiden, The Netherlands

ARTICLE INFO

Article history:
Received 19 January 2010
Received in revised form 15 April 2010
Accepted 16 April 2010

Keywords:
Steel
Failure
Micromechanics
Mechanical characterisation
Electron microscopy
Strain measurement

ABSTRACT

The evolution of local plastic deformation in a dual-phase (DP) steel has been studied using Digital Image Correlation (DIC) and in-situ tensile testing inside a scanning electron microscope. Tests were performed using specially designed samples to study the initiation and evolution of damage in DP1000 steel by measuring the strains at the scale of the microstructure. Micrographs have been analysed using DIC at different stages throughout a tensile test to measure local strain distributions within the ferrite–martensite microstructure. The results show progressive localisation of deformation into bands orientated at 45° with respect to the loading direction. Strain magnitudes are higher in the ferrite phase with local values reaching up to 120%. Several mechanisms for damage initiation are identified and related to the local strains in this steel. The procedure used and the results obtained in this work may help the development of models aimed at predicting the properties of new generation automotive steels.

1. Introduction

Advanced high strength steels (AHSS) deliver greater ductility and formability for equivalent strength levels compared to conventional carbon steels and high strength low alloy (HSLA) grades. The combination of higher strength and better formability provides greater energy absorption capability that improves the crashworthiness of structures made from these steels.

The most common type of AHSS are the dual-phase (DP) steels that are widely used in the automotive industry [1]. DP steels consist of hard martensite islands embedded in a relatively soft ferrite matrix. Damage initiation and development in such two phase material is not well understood and this is a limiting factor in the development and application of future generation automotive steels.

There have been several attempts to investigate the local deformation and its effect on damage of DP and other advanced high strength steels. Ososkov et al. [2] have used in-situ tensile tests to measure local strain partitioning in a DP600 steel before the onset of necking using both Digital Image Correlation (DIC) and a microgrid technique. They interrupted the test regularly in a Scanning Electron Microscope (SEM) to take images and analysed a relatively small area of the microstructure located away from the region of the neck. Following a small number of discrete points located either in the ferrite or in the martensite-rich regions, they also estimated the evolution of local deformation within each region at different locations along the gauge length. They found that the deformation within the martensite-rich regions reached a maximum strain value of 30% while strain values in the ferrite phase increased continuously to over 70% close to the fracture surface. Gerbase et al. [3] investigated the mechanical behaviour of several DP steels with different chemical compositions to study the mechanisms of damage initiation and final failure in these materials. Large plastic strains up to 50% were found in the martensite phase before final fracture by measuring the change of average dimensions of several martensite islands. They reported that damage initiation in these DP steels does not simply occur through void nucleation, but also by decohesion at the interface between the two phases; the latter mechanism playing an important role in the final fracture of the specimens. Kang et al. [4] used DIC to measure strain partitioning in DP600 steel with different tempering conditions. They produced strain maps for the deformed microstructure although the observed covered area was relatively small compared to the scale of the microstructure and some correlation problems occurred at strains above 24%. They studied damage initiation in the two phase microstructures in relation to the average local plastic strain value measured using DIC. However, the area for strain measurements was not large enough to include any damage nucleation sites and therefore local strain values could not be related to the damage initiation sites directly.

The major problem with the microgrid method, despite its accuracy, is its limitation in terms of minimum grid size as it is experimentally challenging to produce microgrids with a submicron pitch. Image correlation techniques have therefore been

* Corresponding author. Tel.: +44(0) 114 222 7862; fax: +44 (0) 114 222 7890.
E-mail address: h.ghadbeigi@sheffield.ac.uk (H. Ghadbeigi).

0921-5093/$ – see front matter © 2010 Elsevier B.V. All rights reserved.
doi:10.1016/j.msea.2010.04.052

Table 1
Chemical composition of the DP1000 steel studied.

C (wt%)	Mn (wt%)	Si (wt%)	Cr (wt%)	V (wt%)	Ni (wt%)	Nb (wt%)
0.152	1.53	0.474	0.028	0.011	0.033	0.014

preferred [5,6] when plastic strains are measured over small gauge lengths.

In this work in-situ micro-tensile tests have been conducted in a SEM chamber to investigate damage evolution in a DP1000 steel in relation to local strain distributions measured using DIC.

2. Experiments

A commercial DP1000 steel grade with 50% ferrite and 50% martensite has been used in this study. The chemical composition of the material is given in Table 1.

The specimen geometry shown in Fig. 1a has been used to obtain the required strain levels given the capacity of the in-situ SEM load frame. Observation of damage initiation is made easier by the small gauge length of the specimen that can be viewed at relatively high magnification of about 50×. All the specimens were manufactured from a 1.5 mm thick sheet with the loading direction parallel to the rolling direction. The samples were mechanically polished and etched first for 5 s in a 2% Nital solution and then for 15 s in a 10% aqueous solution of sodium meta-bisulfite (SMB). The revealed microstructure shows a dark ferrite phase with embedded white martensite islands (Fig. 1b).

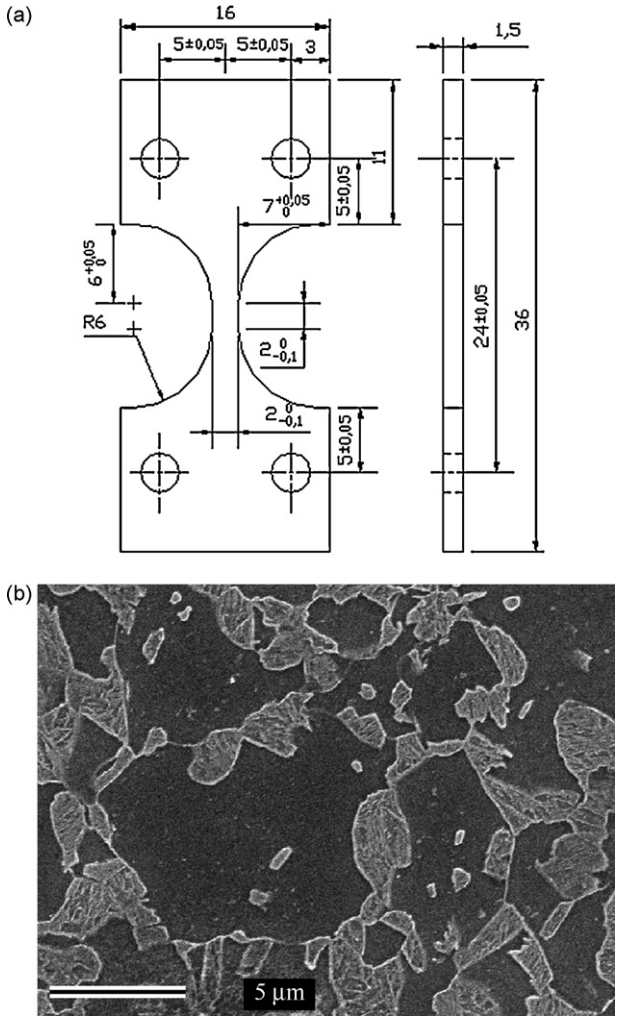

Fig. 1. (a) Micro-tensile test sample and (b) microstructure of DP1000 steel.

A *Deben* MICROTEST tensile stage with a capacity of 5 kN was used to carry out tensile tests. The test machine is loaded in a CAM-SCAN SEM. The test was interrupted regularly during loading to take images of a pre-selected area of the microstructure. This area was located as close as possible to the centre of the gauge length where necking was likely to take place. The tensile test was carried out at a very low strain rate ($\dot{\varepsilon} \approx 0.001\,s^{-1}$) to give sufficient time to capture the deformation of the microstructure and the fracture micro-mechanisms taking place during plastic deformation. Load and displacement of the machine cross head were recorded to produce a stress–strain curve.

DIC was used to analyse the local plastic deformation at the microstructure length scale using micrographs taken during the test. The micrographs were analysed using the commercial image analysis software, DaVIS 7.0, by LAVision [7] to determine the in-plane displacement field from which plastic strain values were calculated. In the current study, the microstructural features of the material have been directly used as the pattern from which to correlate the images between two successive loading steps. Micrographs covering an area of 57 μm × 45 μm were used for the DIC analysis. A multi-pass algorithm [7] leading to a 2.2 μm × 2.2 μm final interrogation window with 75% overlap between windows has been used to make the correlation work. A displacement accuracy of 0.01 pixels was obtained with a strain resolution of about 0.1% [7].

This configuration for the DIC analysis ensures that correlation is found throughout of the selected area.

Correlation results are affected by variations in contrast and brightness as well as by large shape changes of the microstructural features between two successive images. An optimal displacement interval of about 3 μm measured with the LVDT of the tensile stage was finally selected between two loading steps in order to obtain successful results. The test was stopped prior to the final fracture of the specimen as a result of increased surface roughness due to inhomogenous out of plane deformation of the ferrite and martensite regions leading to a loss of correlation.

3. Results

Fig. 2 shows the engineering stress–strain curve obtained from the test. Average engineering strain values within the gauge section were determined using the displacement measured using a LVDT and the initial gauge length. Point A corresponds to the onset of softening and Point B corresponds to the last micrograph taken before fracture of the specimen that took place at a strain value of 52%. The small stress variations along this curve correspond to the interruption of the test needed to take the micrographs for DIC analysis.6

3.1. Damage evolution

The recorded micrographs have been used to study the development of localised deformation as well as damage initiation and propagation. An example of this is shown in Fig. 3 by comparing the micrographs taken before and after deformation. The first appearance of non-uniform deformation was clearly observed on these micrographs after an applied strain value of 22% with the formation of localised deformation bands detected within large ferrite grains (Fig. 3d), as opposed to the smaller ferrite regions trapped between martensite islands.

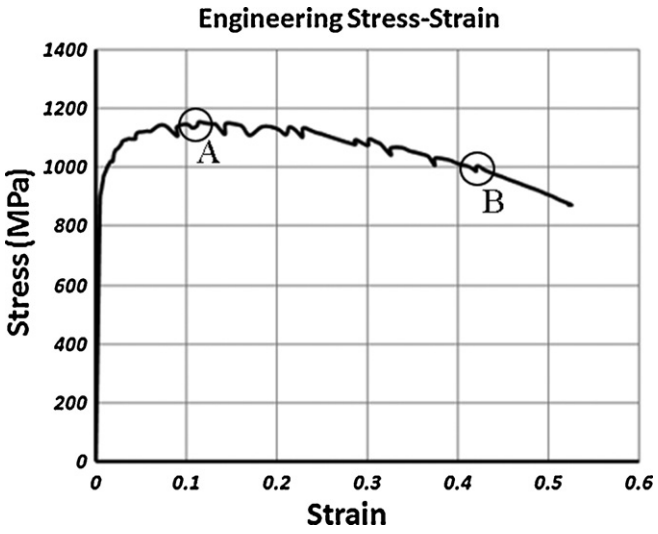

Fig. 2. Engineering stress–strain curve of material tested in-situ. Note that the large amount of post-uniform elongation is due to the tensile geometry.

Localisation of plastic deformation at the ferrite–martensite interface was noticed at larger applied strain values. Fig. 4a and b shows such localisation leading to progressive damage formation (within the triangle) for an applied strain of 29% and 42% respectively. These areas are enlarged in Fig. 4c and d shows more clearly the propagation of damage through both the ferrite and martensite phases. Localised deformation bands within large ferrite phases (areas in rectangle shown in Fig. 4) were also more intense as the applied strain increased. Separation of two martensite islands was also observed in the region within the circle in Fig. 4b as a result of localised deformation in the ferrite phase.

3.2. Strain measurement

Distribution of the microscale strain component ε_{yy}, in the loading direction, is shown in Fig. 5 for increasing applied strain values. The maps on this figure are superimposed onto the SEM micrographs of the deformed microstructure. Localisation of deformation in the microstructure starts to be clearly observed for an applied strain of 22% with the formation of deformation bands within the rectangle shown in Fig. 5a (light blue regions). The bands initiate inside the ferrite, but then cross martensite islands as they develop. Strain magnitude within the bands as well as the band density increases as the applied strain increases (Fig. 5b–d). The highest strain intensities within these bands are shown in the highlighted areas of Fig. 5d with values up to 130% locally for an applied strain of 42%. These values are located in the ferrite phase, but very close to the interface with the martensite.

A detailed analysis was then carried out to quantify strain distribution within each phase in the selected area for DIC analysis. A plot of the distribution of strain values is shown for each phase in Fig. 6a. The frequency of strain values normalised by the total number of data points in each phase shows a bell-shaped distribution with mean values of 35% in the ferrite phase and 25% in the martensite phase. In these graphs, the pixels located along the phase boundaries have been removed from the analysis to minimise errors. These results show that the martensite phase experiences large plastic deformation during the tensile test with local strain val-

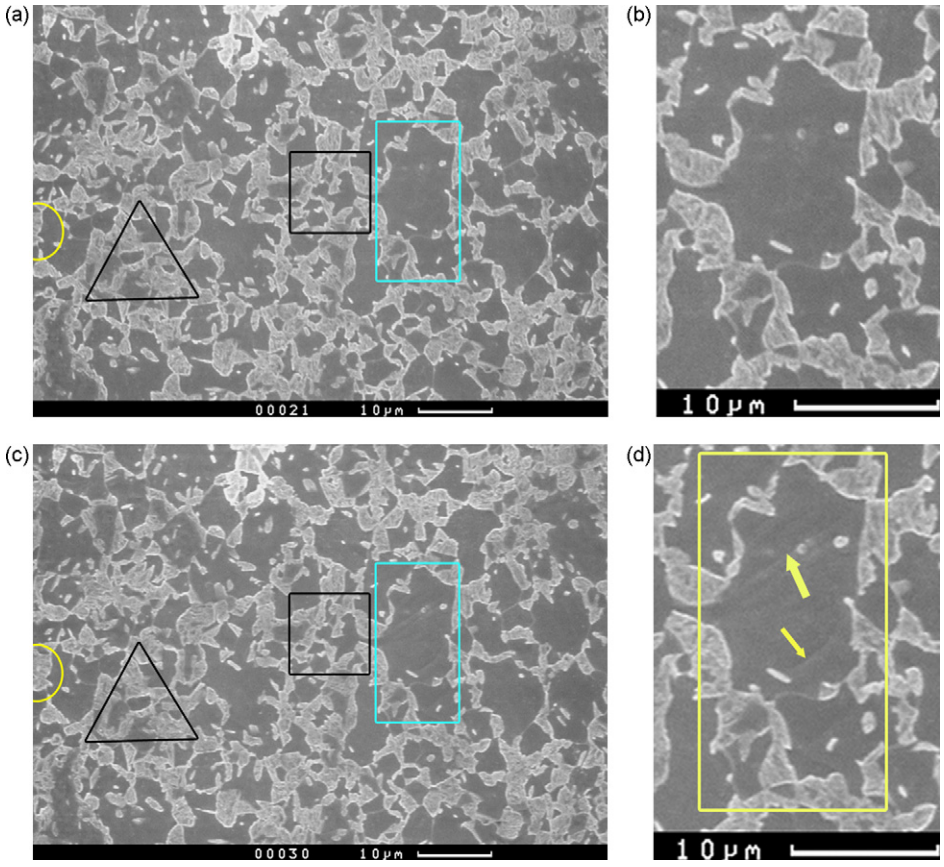

Fig. 3. Area analysed with DIC. (a) Deformed microstructure after an applied strain of 18%. (b) Close-up view of the area within rectangle in (a). (c) Deformed microstructure after an applied strain of 22%. (d) Formation of deformation bands in the same rectangular area (the tensile direction is vertical on these pictures).

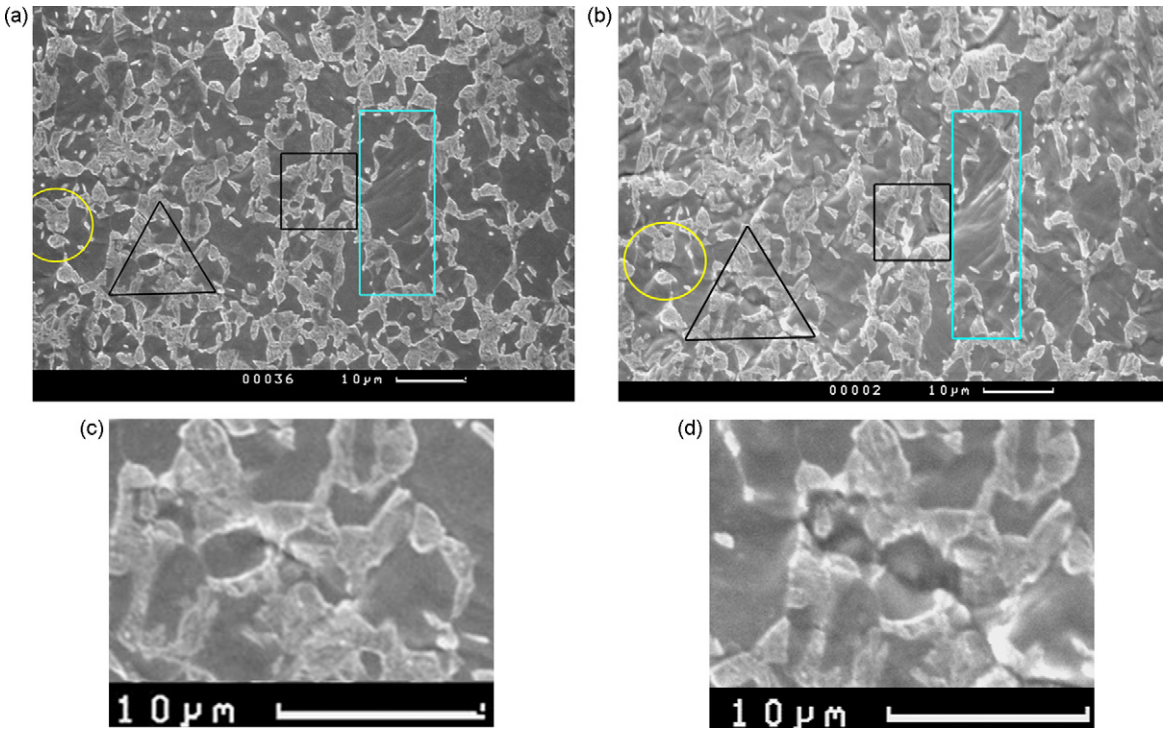

Fig. 4. Deformed microstructure (a) after 29% and (b) 42% applied strain with (c) and (d) showing a close-up view of the area within the triangle shown in (a) and (b) respectively.

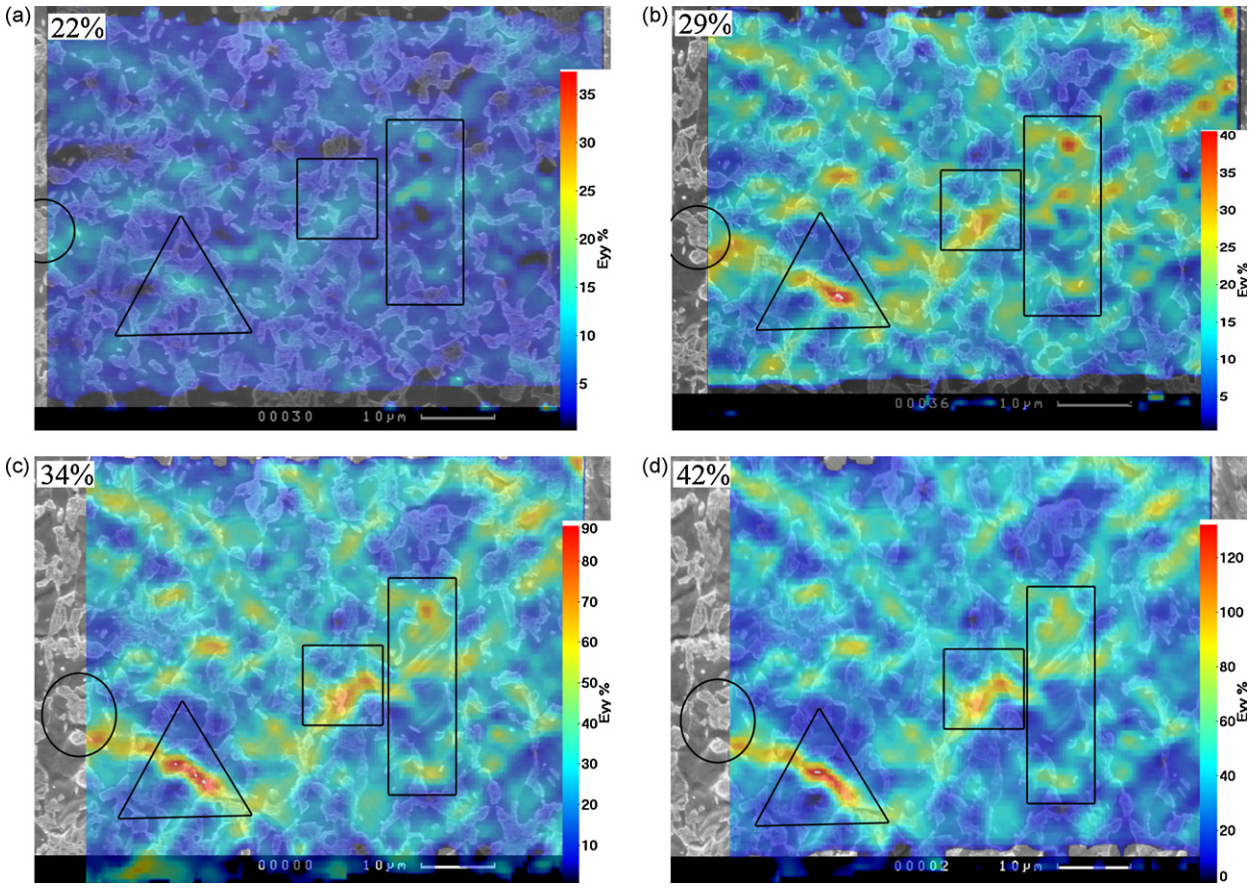

Fig. 5. Plastic strain evolution within the microstructure of DP1000 during the tensile test.

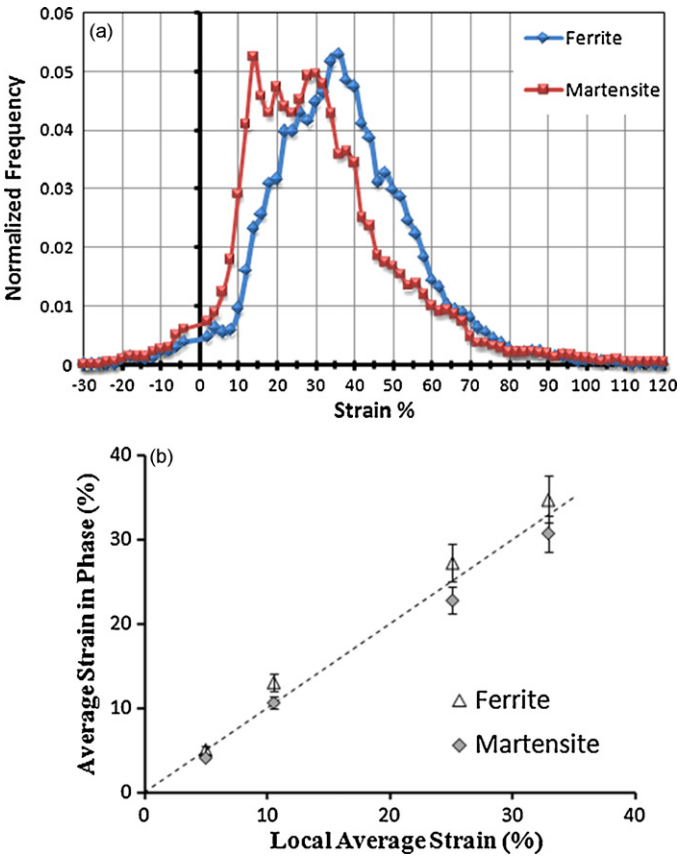

Fig. 6. (a) Distribution of plastic strain in each phase before final fracture and (b) evolution of strain partitioning during the test.

ues up to 110% for an applied strain of 42%. The evolution of strain partitioning within the two phases during the test has also been quantified. Results are shown in Fig. 6b where the strain values measured from the overall deformation of the selected area for DIC analysis has been considered as the local average strain. Results show that even though the ferrite phase deforms slightly more than the martensite phase, strain partitioning is very similar between the two phases throughout the test.

The large plastic deformation of martensite has been verified by estimating the overall shape change of two martensite islands shown in the highlighted squares of Figs. 3 and 4. Fig. 7a and b shows the highlighted boundaries of these martensite islands in the undeformed and deformed configurations respectively. The boundaries of the deformed and undeformed martensite islands (M1 and M2) are superimposed in Fig. 7c in order to estimate the overall elongation. Measurement results show that the islands M1 and M2 elongate by 51% and 30% respectively which is in agreement with the large strain values measured with DIC.

4. Discussion

Results from the micro-tensile test carried out on DP1000 have shown the evolution of local deformation taking place at the scale of the microstructure up to the final fracture of the specimen. Local strain heterogeneity starts to be clearly visible using DIC after 22% applied strain and becomes more pronounced up until the end of the test (Fig. 5). Fig. 5a shows that localised bands of deformation start forming with the highest strain values located either inside large ferrite islands or very close to the interface between ferrite and martensite for small ferrite islands trapped between several islands of martensite. These bands orientated at about 45° with respect to the loading direction follow a path lying mostly within ferrite areas, but also crossing martensite islands. As the applied strain increases the localisation of deformation within these bands becomes more intense reaching values up to 130% (Fig. 5d). The orientation of these bands corresponds to the orientation of slip bands clearly observed in the ferrite phase in Figs. 3d and 4b, which seems to indicate that the initial phase of the formation of these bands is related to the plastic deformation mechanisms that operate within the ferrite grains.

Results from Figs. 4 and 5 show the large deformation experienced by the microstructure at the surface of the specimen with relatively few damage sites visible by the end of the test. As clearly shown in Ref. [8] the volume fraction of voids is much higher at mid-thickness of the specimen due to higher stress triaxiality at that location. This explains why the fracture of the specimen is suddenly observed due to the emergence of a large crack which initiated below the surface. The results therefore show that the interface between ferrite and martensite is very strong, probably due to its cohesive nature as reported in Ref. [9] for DP steels. The high strain values measured in areas close to the interface between the two phases (Fig. 5d) are in line with values of 100% measured at the interface of the two phases in Ref. [4].

Several mechanisms have been observed for the early stages of damage appearance in the analysed microstructure. Fig. 8a shows a close-up view of the square area in Fig. 4b with damage taking place in the ferrite phase after large plastic deformation and a corresponding local strain value of 120%. This particular void growth mechanism has also been reported in Ref. [4] for DP600. A detailed observation of the microstructure and its evolution during the test reveals that a more frequent damage mechanism corresponds to crack initiation at the interface between ferrite and martensite (Fig. 8b) due to the incompatibility of plastic deformation locally between the two phases. The crack, then, propagates nearly perpendicular to the interface through the martensite phase then follows at or near the narrowest part of a martensite ligament (Fig. 8c). Propagation may then extend into the neighbouring ferrite phase as shown in Fig. 4d.

Fracture of the martensite phase has also been reported in other studies on DP steels [10–12]. However the mechanism of fracture by decohesion at the interface between ferrite and martensite reported in Refs. [3,4,12] has not been observed in this work. Fig. 4b also shows the separation of two initially connected martensite islands in the highlighted circular area, which is a mechanism reported in Refs. [4,12]. This mechanism might be due to either the failure of a prior austenite grain boundary or the fracture of martensite islands following the mechanism previously mentioned.

The graphs shown in Fig. 6 quantify the distributions of strain values within the two phases measured with DIC during the test. Both phases show similar strain distributions (Fig. 6a) with a slightly higher mean value for the ferrite phase and local strain magnitudes up to 110% after removing the pixels located along the interfaces to minimize errors. The martensite islands in DP1000 can therefore accommodate very large deformation without failure with a mean value which is comparable to the value of 30% reported in Ref. [4] for DP600. However local strain values as high as 110% have not been reported elsewhere. The strain distributions between ferrite and martensite remain similar throughout the test with a slightly higher average strain value in the ferrite (Fig. 6b). Given the errors introduced in the calculation of average strain values per phase by removing the pixels located along the phase boundaries in the strain analysis, the results show almost one to one correspondence with the local average strain up until the end of the test.

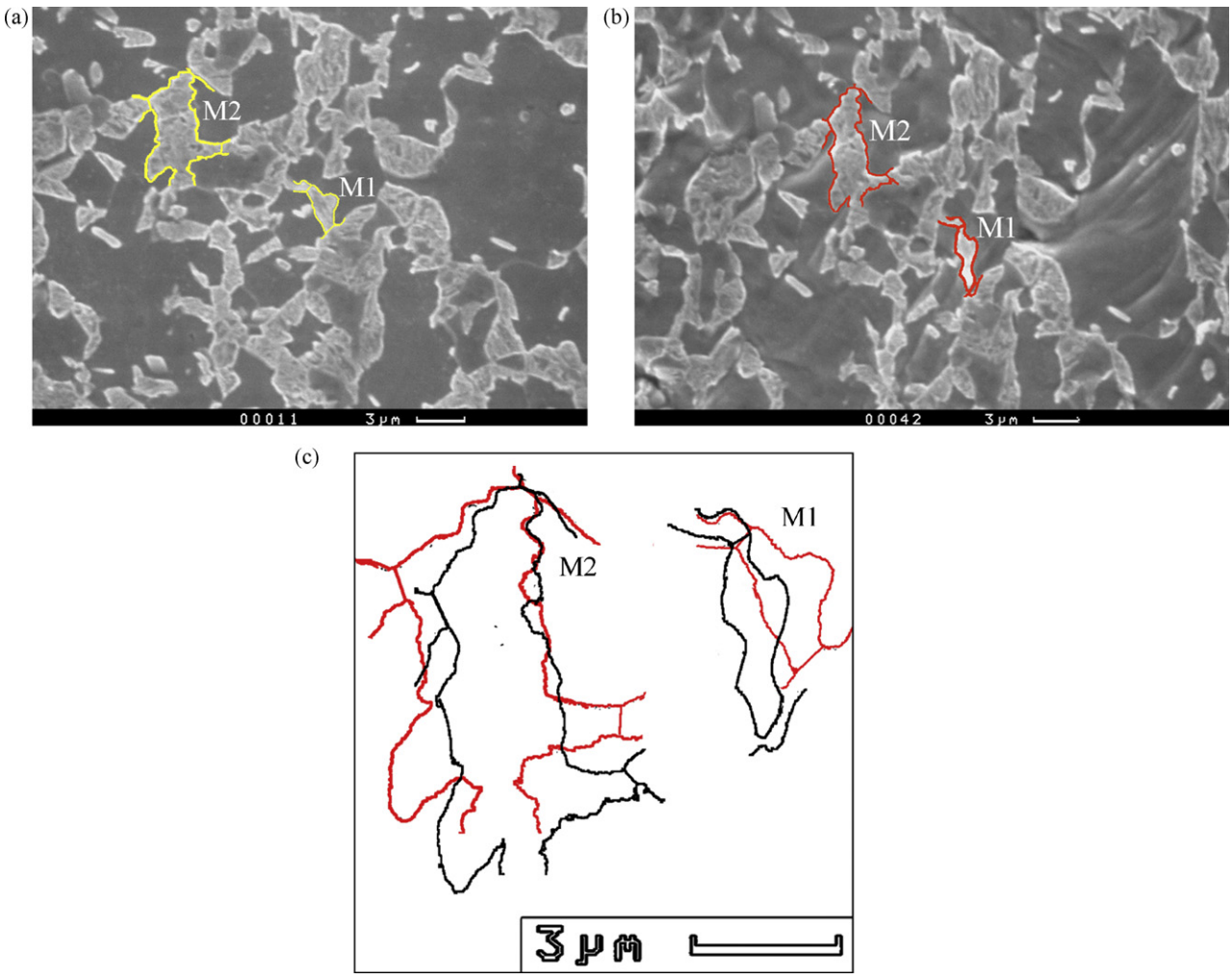

Fig. 7. Highlighted martensite islands in the (a) undeformed and (b) deformed microstructures and (c) superimposition of the boundaries for quantification of the phase elongation.

Our findings differ from the results reported by Ososkov et al. [2] for DP600 with the martensite-rich regions saturating at a strain value of 30% while the ferrite phase reached strain values of 80% at the end of the test. This is likely to be due to the different microstructures and carbon contents of the phases for these two DP steels. The differences may also be influenced by the methods used in characterising strain partitioning since the average strain values shown in Fig. 6b are statistically more meaningful than the single point measurements reported in Ref. [2] at various locations along the gauge length.

The combination of DIC results obtained over a relatively large area of the microstructure combined with the observation of damage development on the same area therefore provides new insight into the effect of the heterogeneity of deformation that takes place

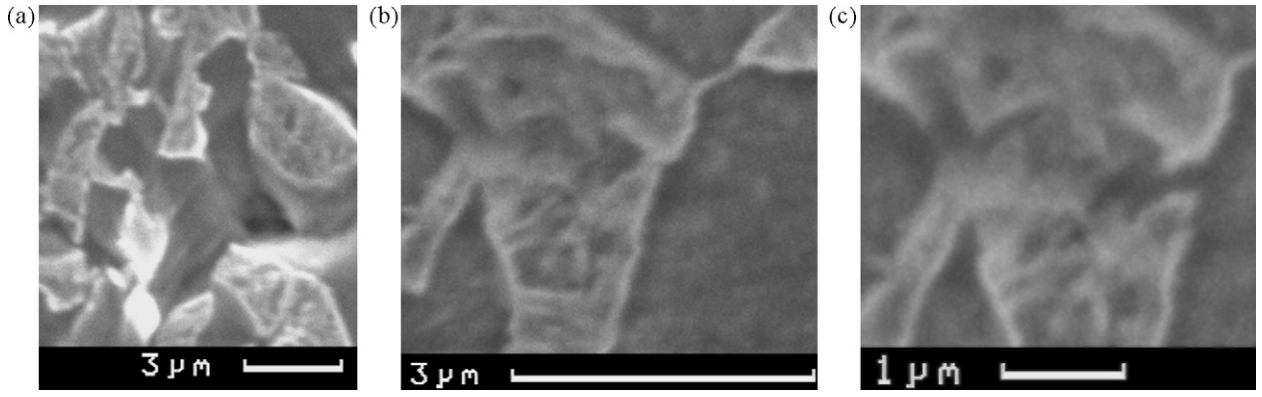

Fig. 8. (a) Enlarged micrograph of the square area of Fig. 4 showing damage nucleation in the ferrite phase, (b) damage initiation at the ferrite–martensite interface and (c) crack propagation into the martensite island.

at the scale of the microstructure on the formation of damage for DP steels. Strain analysis results for this representative area of the microstructure can also be used to develop and validate physically based scale-transition models of these two phase materials with the aim of predicting the properties of new generation automotive steels from their local behaviour.

5. Conclusion

An in-situ micro-tensile test has been carried out on a DP1000 grade steel in order to measure the local plastic strain distributions in the ferrite and martensite phases and their evolution for a better understanding of damage nucleation. Digital Image Correlation has been used to quantify the local strain values using a sequence of successive images recorded during the test. Results have shown a very heterogeneous strain distribution within the microstructure with a localisation of deformation into bands orientated at 45° with respect to the loading direction and maximum strain values up to 130% for an applied strain of 42%. Several damage mechanisms have been observed depending on the local configuration of the microstructure: damage in the ferrite by void nucleation and growth for strain values of about 120%, fracture and separation of martensite islands and decohesion at the interface between ferrite and martensite after strain values as high as 130%.

Acknowledgements

The authors would like to thank EPSRC (grant number EP/F023464/1) for financial support and CORUS RD&T, IJmuiden in the Netherlands for providing the material of this study.

References

[1] T. Senuma, ISIJ Int. 41 (2001) 520–532.
[2] Y. Ososkov, D.S. Wilkinson, M. Jain, T. Simpson, Int. J. Mater. Res. 98 (2007) 664–673.
[3] J. Gerbase, J.D. Embury, R.M. Hobbs, in: R.A. Kot, J.W. Morris (Eds.), Structures and Properties of Dual Phase Steels, AIME, New York, 1979, pp. 118–143.
[4] J. Kang, Y. Ososkov, J.D. Embury, D.S. Wilkinson, Scripta Mater. 56 (2007) 999–1002.
[5] H. Jin, W.-Y. Lu, J. Korellis, J. Strain Anal. Eng. Des. 43 (2008) 719–728.
[6] M.A. Sutton, N. Li, D.C. Joy, A.P. Reynolds, X. Li, Exper. Mech. 47 (2007) 775–787.
[7] LAVision, DaVis Strain Master Software, 2005.
[8] E. Maire, O. Bouaziz, M. Di Michiel, C. Verdu, Acta Mater. 56 (2008) 4954–4964.
[9] J.Y. Koo, G. Thomas, in: A.T. Davenport (Ed.), Formable HSLA and Dual-phase Steels, AIME, New York, 1977, pp. 40–55.
[10] M. S. Rashid, Paper 760206, Soc. Auto. Eng. Cong, Detroit, 1977, pp. 938–949.
[11] T. Gladman (Ed.), The Metallurgy of Microalloyed steels, The Institute of Materials, The University Press, London, 1997.
[12] D.L. Steinbrunner, G. Krauss, Metall. Trans. 19 (1988) 1821–1826.